Proceedings of the 25th International Conference on
Port and Ocean Engineering under Arctic Conditions
June 9-13, 2019, Delft, The Netherlands

Validation of the line-like nature of ice-induced loads using an inverse method

Jillian M. Adams[1], Ville Valtonen[1], Pentti Kujala[2]
[1] Aker Arctic Technology Inc., Helsinki Finland
[2] Aalto University, Espoo, Finland

ABSTRACT

Throughout the last 50 years, knowledge of ship-ice interaction and the mechanics of the ice breaking process has improved through numerous full-scale studies; however, the understanding of precise ice-induced pressures and load heights requires further refinement to design safer, more efficient ships.

During its construction, the hull structure of the oblique icebreaker *Baltika* was instrumented with strain gauges. The sensor arrangement was designed to allow the measurement of the vertical distribution of ice loads and the ice-induced load patch height. Two years of data have been gathered during operations in the Russian Arctic.

An inverse method was developed to study the applied ice-induced loads and the load patch on the ship's hull. The method utilises an influence coefficient matrix to describe the structural response to an applied load. Using FEM, strain response functions are fitted at each sensor location to generate the terms of the influence coefficient matrix. An optimisation routine solves the inverse equation and determines the magnitude of the applied pressure and the height of the load patch.

Using the full-scale measurements recorded on board the *Baltika,* the development of the ice pressure from first contact to load disengagement was studied for individual ice impact events. The analysis revealed that the structures experienced concentrated, high pressure loads during impact events. The results confirmed that ice-induced loads are line-like in nature.

KEY WORDS: Ship-ice interaction; Inverse method; Full-scale measurement; Ice-induced load; Arctic.

INTRODUCTION

Ship-ice interaction is a complex phenomenon that has interested researchers for many years. As new shipping routes open in the Arctic, a need arises to develop safer, more efficient ships to operate in these remote areas. The study of full-scale measurements is fundamental to expanding the scientific knowledge concerning ship-ice interaction.

Since the 1970s, many full-scale measurement campaigns have been carried out in various ice-infested waters (Suominen, 2018). Their results have contributed to the advancement of the rules governing the design of ice-going vessels through improving the understanding of failure mechanics and induced forces during ship-ice interaction. Some examples include a study of the relationship between ice thickness and induced forces on the Norwegian *KV Svalbard* (Leira, et al., 2009), a study of the influence of load length on the magnitude of loads (Suominen & Kujala, 2015), and a study aimed to estimate maximum ice-induced loads on board the *CCGC Terry Fox* (Gagnon, 2008).

One aspect of ice class rules that has changed significantly over the course of the 20th century is the height of the load patch induced during ship-ice interaction. The best example of this development is found in the Finnish-Swedish Ice Class Rules (FSICRs). In the 1970s, the height of the load patch was assumed to be the same as the ice thickness. In the 1985 revision of the rules, the load height was reduced to 20-40% of the design ice thickness, and this load height is reflected in the current rules (Riska & Kamarainen, 2011). However, studies on board the Finnish Icebreaker Sampo in the early 1990s observed narrow line-like contacts with high ice pressures (Riska, 1991). The history reduction of design load heights is illustrated in Figure 1.

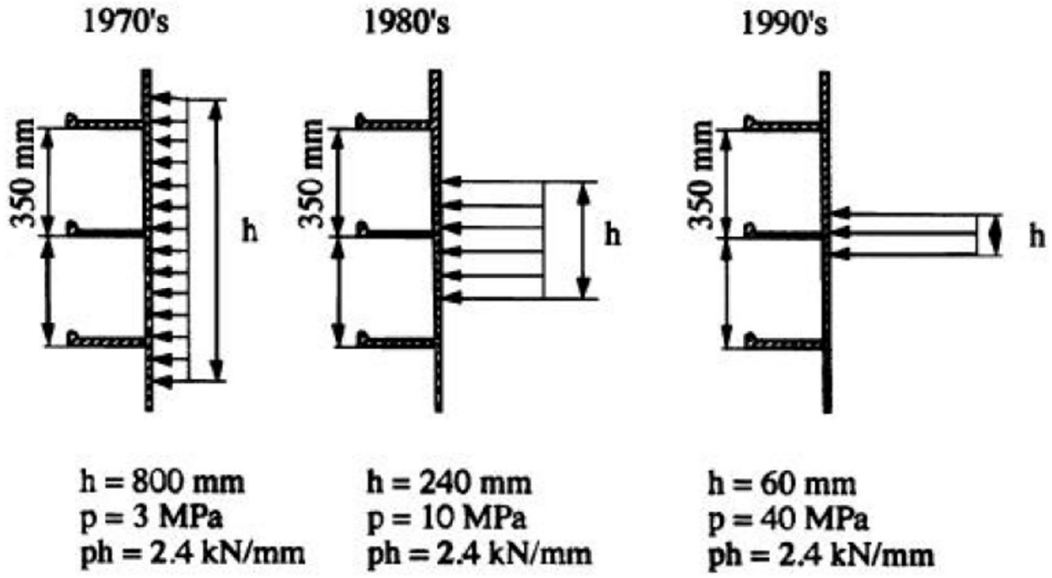

Figure 1. Historical developing of ice load design heights (Kujala, 2017)

The objective of this study is to investigate the load height of ice-induced loads using an inverse method. Full-scale measurements taken on board the icebreaker *Baltika* while operating in the Gulf of Ob are analyzed.

Multipurpose Emergency and Rescue Vessel *Baltika*

The *Baltika* was built in 2014 as an icebreaking multipurpose emergency and rescue vessel. The ship is classed as Russian Maritime Register of Shipping (RMRS) Icebreaker6 and is equipped with three 2.5 MW azimuthing thrusters. The *Baltika* is a unique vessel that is capable of breaking ice using its inclined port side, in addition to a traditional double acting hull. It is, therefore capable of breaking a 40-50 m wide channel, despite only having a beam of 20.5 m. To gain a better understanding of the loads induced on its unique hull form, the *Baltika* was instrumented for full-scale measurements. Figure 2 depicts the location of the sensors installed on the *Baltika* and Table 1 gives the main dimensions of the ship.

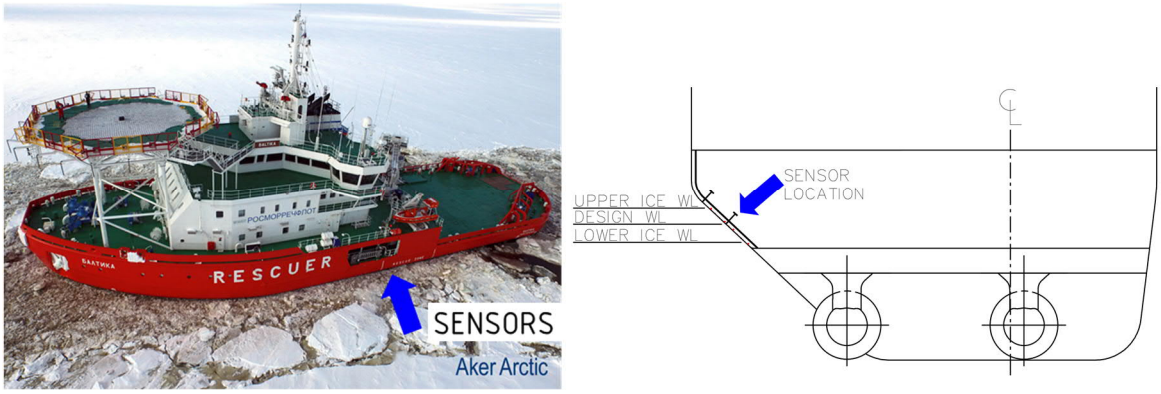

Figure 2. Sensor location on board the *Baltika*

Table 1. Main dimensions of the *Baltika*

Characteristic	Dimension	Unit
Length	76.4	m
Beam	20.5	m
Draft	6.3	m
Power	3 x 2.5	MW
Speed	15.4	kn
Ice Class	RMRS Icebreaker6	--

The strain sensors are distributed about the design waterline on the inclined side of the ship, near midship. There is a total of 22 sensors installed which are distributed between 5 shear strain sensor pairs and 12 normal strain sensors. The shear strain sensors are positioned on the neutral axes of two frames and the waterline stringer while the normal strain sensors are located at the center of the plate fields. The sensor arrangement was designed to have a high number of sensors in the vertical direction as shown in Figure 3.

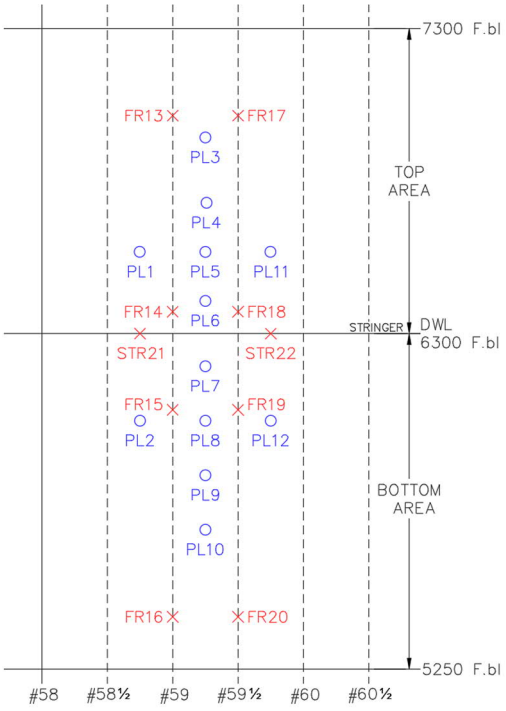

Figure 3. Positions and names of the strain gauges

METHODOLOGY

Inverse Methods

In engineering, an inverse problem is when the system's response is known, but the inputs, and often the boundary conditions, are unknown. The nature of full-scale strain measurements on board ships is inherently inverse: the strain response of the ship's structures is measured; however, the load that caused the deformation is unknown. As such, inverse methodologies must be used to determine the inputs.

Due to the lack of known inputs and boundary conditions of inverse problems, one common issue is their 'ill-posedness', meaning a unique solution might not exist for all data measurements. To solve an 'ill-posed' problem, regularisation methods are employed. Uhl (2007) composed a review of regularisation methods and their applications in inverse engineering. One of the most common and effective methods is the Tikhonov regularisation method (Tikhonov & Arsenin, 1977). Equation 1 presents the inverse equation for the forward force-strain relationship (Equation 2) including Tikhonov's regulation.

$$argmin_f\{\|\boldsymbol{Zf} - \boldsymbol{\varepsilon}(t)\|^2 + \lambda \|\boldsymbol{Hf}\|^2\} \quad (1)$$

$$\boldsymbol{\varepsilon} = \boldsymbol{Zf} \quad (2)$$

In Equation 1, $\boldsymbol{Z}$ represents the influence coefficient matrix that relates the system's inputs and outputs, $\boldsymbol{\varepsilon(t)}$ and $\boldsymbol{f}$ are the system's strain inputs and load outputs, respectively, $\boldsymbol{\lambda}$ is Tikhonov's regularisation parameter, $\boldsymbol{H}$ is a smoothing matrix and $\|\cdot\|$ is the Euclidean norm. The regularisation parameter must be chosen carefully as it has a large influence on the results. A study of line-loads on paper rollers observed that the regularisation introduced error to the inverse solution when solving simple force determination problems (Romppanen, 2008).

Similarly, Ikonen concluded in his work on ice-induced loads that the solution was not compromised when the regularisation parameter had a value of 0 and the inverse problem was simple (Ikonen, 2013). For this study, a regularisation parameter of 0 is chosen since the inverse method only solves for 4 variables.

The inverse load determination problem is classified as a multi-objective minimisation problem. It is subjected to linear constraints and the variables are bounded. The optimisation is done using Matlab. For each impact event the strain history of the desired period is used as input into the optimisation routine. The second input of the inverse problem is the influence coefficient determined through a finite element model of the ship's structure. An outline of the methodology is found in Figure 4.

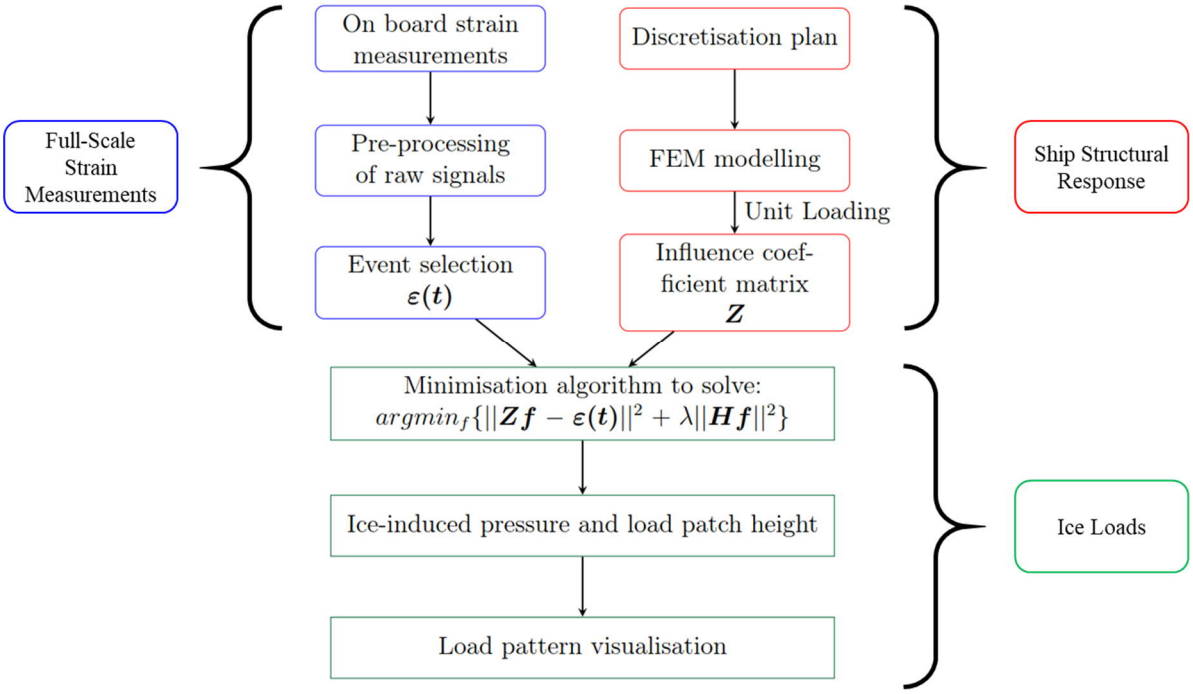

Figure 4. Flow chart of the methodology

Discretisation of the Solution Area

The instrumented area on board the *Baltika* (Figure 3) must be discretised to solve the inverse force-strain equation. The high density of sensors in the vertical direction is favourable for investigating the height of the load patch, in addition to the magnitude of the pressure load on the ship's shell. The discretisation pattern was developed to be flexible in the load patch dimensions, such that the height of the load patch is variable. However, the load height is assumed to be constant across the frame spacing.

The large stringer, found at the ship's waterline, created a challenge in the solution process of the inverse problem. The stringer is significantly more rigid than the surrounding structure, creating a discontinuity. The solution area was, therefore, divided into two areas: Solution Area 1 is above the stringer and Solution Area 2 is below the stringer. Figure 5 presents the discretisation pattern and the bounds of the variables. It was assumed that only one area was loaded at a time and therefore only the maximum pressure between the two Solution Areas was analysed.

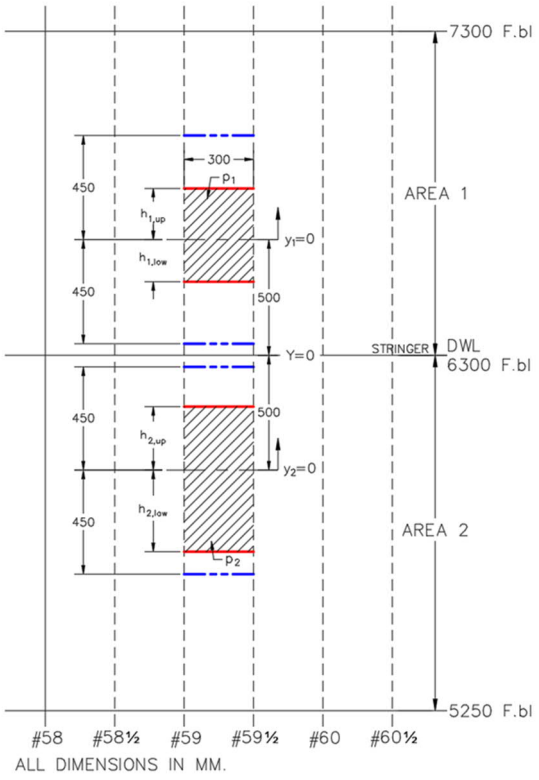

Variable	Lower Bound *	Upper Bound *	Unit
$h_{1,up}$; $h_{1,up}$	+0.05	+0.95	m
$h_{2,up}$; $h_{2,up}$	-0.95	-0.05	m
p_1; p_2	0	50	MPa

*Relative to Y=0

Figure 5. Discretisation of the solution area

Influence Coefficient Matrix

The influence coefficient matrix (ICM) from Equation 2 describes the strain response of the ship's hull structure at the sensor locations in response to unit loads. In its most basic form, the elements of the ICM can be described using Equation 3, where Z_{ij} is the response of the *i*th senor to a pressure load on the *j*th discretisation area. However, due to the fluctuating height, the response of the system becomes a function of the height of the load patch and each term of the ICM is a polynomial response function. The response at sensor *i* to a pressure load on area *j* with vertical boundaries of $y_j = 0$ and the *k* (upper or lower) height variable is described by Equation 4, where c_i are the polynomial coefficients for the *i*th sensor.

$$Z_{ij} = \frac{\varepsilon_i}{p_{unit_j}} \tag{3}$$

$$Z_{ij}(h_{jk}) = c_{i,0} + c_{i,1}h_{jk} + c_{i,2}{h_{jk}}^2 + .. + c_{i,m}{h_{jk}}^m \tag{4}$$

Finite element analysis was used to determine the strain response of the ship's structure. The extent of the model was determined by the closest rigid structure, namely decks and bulkheads. A mesh independence study was conducted as part of the method verification process (Adams, 2018). Figure 6 presents the extents of the FE model as well as a sample load patch and the location of fixed boundary conditions. The influence of pinned or fixed boundary conditions of the FE model was studied by Ikonen (2013).

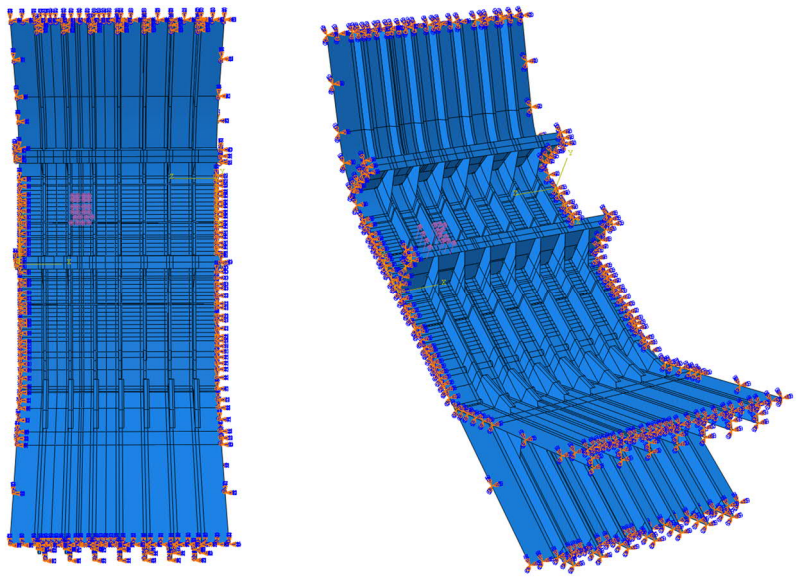

Figure 6. Finite element boundary conditions and sample load patch

The linear nature of the finite element model (FEM) solver used to determine the strain responses of the ship's structure allows for several simplifications of the response functions. The principle of superposition can be used to combine the response of the structure to the upper and lower height variables in each respective Solution Areas, as shown in Equation 5. Furthermore, based on the pressure definitions shown in Figure 7, the response of the structure to the varying upper variable is the opposite of the response to the lower height variable as described in Equation 6.

$$Z_{ij}(h_j) = Z_{ij}(h_{j,up}) + Z_{ij}(h_{j,low}) \tag{5}$$

$$Z_{ij}(h_{j,up}) = -Z_{ij}(h_{j,low}) \tag{6}$$

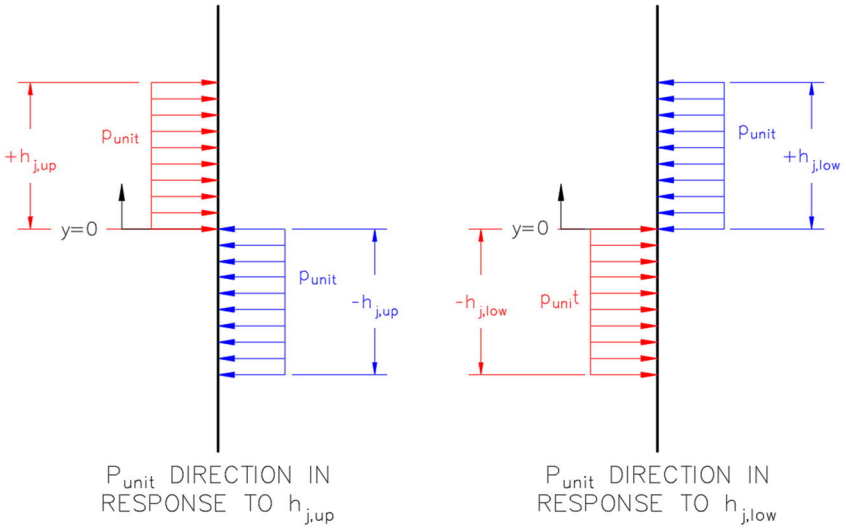

Figure 7. Definition of directions for unit pressures for varying load heights

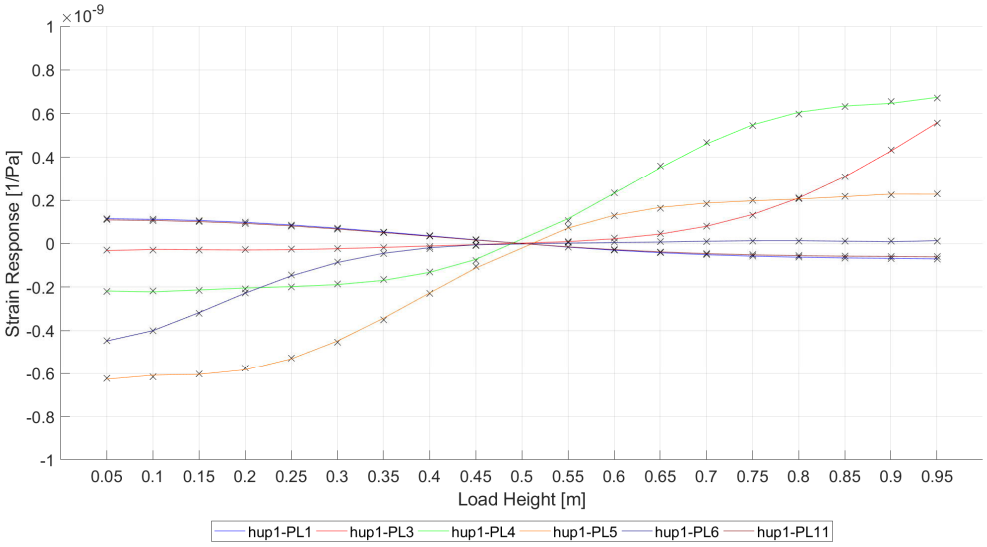

Figure 8. Sample strain response curves for variable $h_{1,up}$

The final form of the elements of the ICM are given in Equation 7, where $c_{i,m}$ are the polynomial coefficients for the curved-fitted 6th order polynomial. A sample of strain functions for the normal sensors in Solution Area 1 is given in Figure 8. Equation 8 is the final ICM used in the inverse solution.

$$Z_{ij}(h_{j,up}, h_{j,low}) = \begin{bmatrix} c_{i,1} & c_{i,2} & \dots & c_{i,m} \end{bmatrix} \begin{Bmatrix} (h_{j,up} - h_{j,low}) \\ (h_{j,up} - h_{j,low})^2 \\ \vdots \\ (h_{j,up} - h_{j,low})^m \end{Bmatrix} \tag{7}$$

$$\boldsymbol{Z}(h) = \begin{bmatrix} Z_{1,1}(h_{1,up}, h_{1,low}) & Z_{1,2}(h_{i,up}, h_{i,low}) \\ Z_{2,1}(h_{2,up}, h_{2,low}) & Z_{2,2}(h_{2,up}, h_{2,low}) \\ \vdots & \vdots \\ Z_{17,1}(h_{17,up}, h_{17,low}) & Z_{17,2}(h_{17,up}, h_{17,low}) \end{bmatrix} \tag{8}$$

Event Selection

Two representative sets of ice-impact events were selected from the two years of measurement data. The first set of 250 events was selected from the upper 66% of hourly maximum strain measurements on normal sensors PL3-PL10. The 250-event set was used for the general analysis to gather information and statistics surrounding the occurrence of peak pressure loads. A period of 0.1 seconds, centred about the occurrence of peak strain measurement, was considered for the analysis. Figure 9 presents the distribution based on location of the selected impact events analysed in the general analysis.

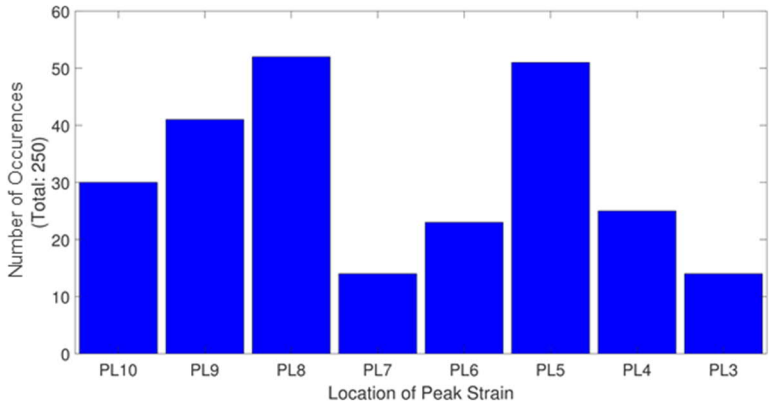

Figure 9. Distribution of events selected for the general analysis

The second set, used for the detailed analysis, was selected from both the normal and shear sensors. A total of 102 impact events were selected from the upper 50% of strain measurements: 52 based on shear strain measurements and 50 from normal strain measurements. A duration of 1 second was extracted from the raw data for analysis. Figure 10 presents the distribution of events selected for the detailed analysis.

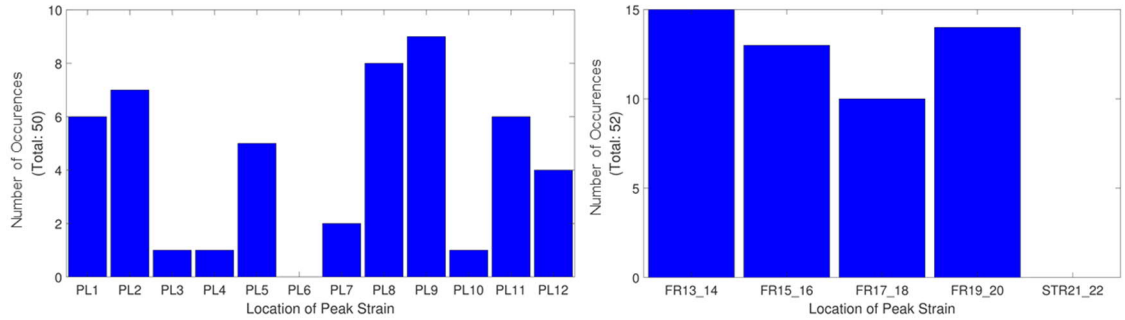

Figure 10. Distribution of events selected for the detailed analysis based on normal and shear strain measurements (left and right, respectively)

RESULTS

General Impact Event Analysis

Of the 250 events selected for analysis, the results of 166 impact events are presented and further analysed. The solution for the remaining 84 events did not converge within the limits of the optimisation routine. Figure 11 presents the distributions of the peak pressures from the impact events and the load heights. The maximum pressure incurred during the selected ice impact events is most often between 10 and 25 MPa. This range accounts for 84% of the selected events.

Only 4 events resulted in pressures above 25 MPa, indicating that the pressure distribution follows an exponentially decaying trend. This aligns with findings in the literature that extreme ice loads follow exponential-type trends (Ochi, 1981) (Suominen, 2018) (Kujala & Vuorio, 2009).

The histogram of load heights (Figure 11) indicates that the contact area between the ship's hull and the ice floe is narrow. Only 12 of the 166 impact events had load heights greater than 5 cm. Most impact events studied had load heights on the order of 1-2 cm, which creates a more concentrated load that assumed in the design rules. The narrow, line-like nature of the ice loads corresponds well with the visual observations made on board the *IB Sampo* in the 1990s (Riska, et al., 1990).

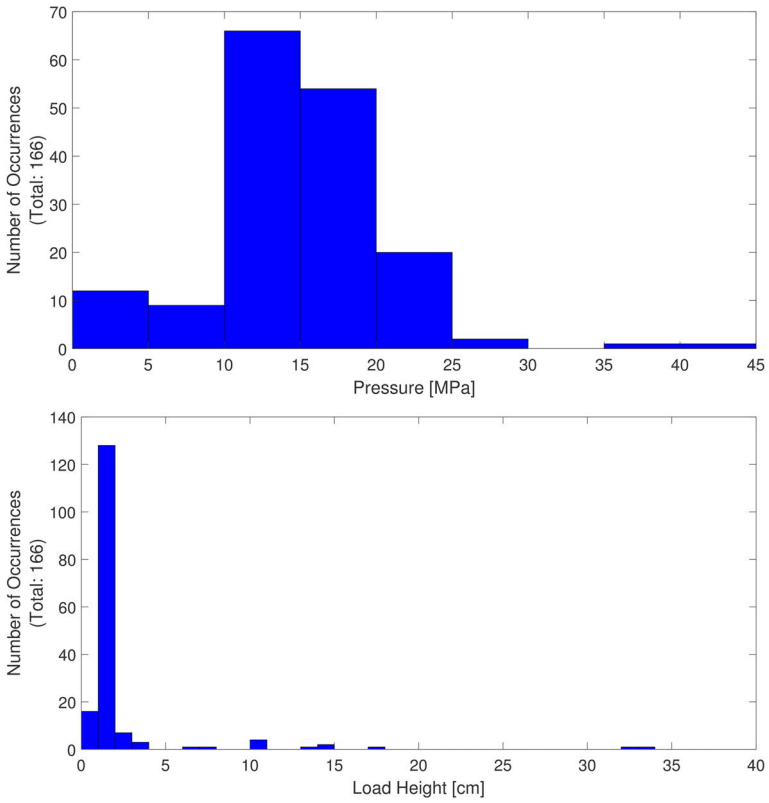

Figure 11. Distribution of pressure (top) and load height (bottom) at occurrence of maximum impact

Detailed Event Analysis

A detailed analysis of 102 impact events was undertaken to understand the development of pressure and load patch height throughout the ship-ice interaction. The induced line-load, pressure and load height were examined for a 1-second period for each impact event. Figure 12 presents the histories for two events: one is a simple event where only one sensor was loaded and the second shows an impact event where the ice load moves during the interaction.

The results from Event 9 shows clear development of pressure as the ice comes into contact with the hull. The load height, however, is markedly constant throughout the duration of the impact event. The load height is approximately 2 cm at the time of maximum pressure. Event 9 shows a distinct line-like load patch.

In contrast, the ice load patch induced during Event 54 is more dynamic. The ice floe is shown to be moving downward throughout the interaction as can be seen in the load patch samples in Figure 12. The strain history reflects this behaviour as two sensors show consecutive pressure peaks. Two pressure peaks of approximately 10 MPa are experienced during Event 54.

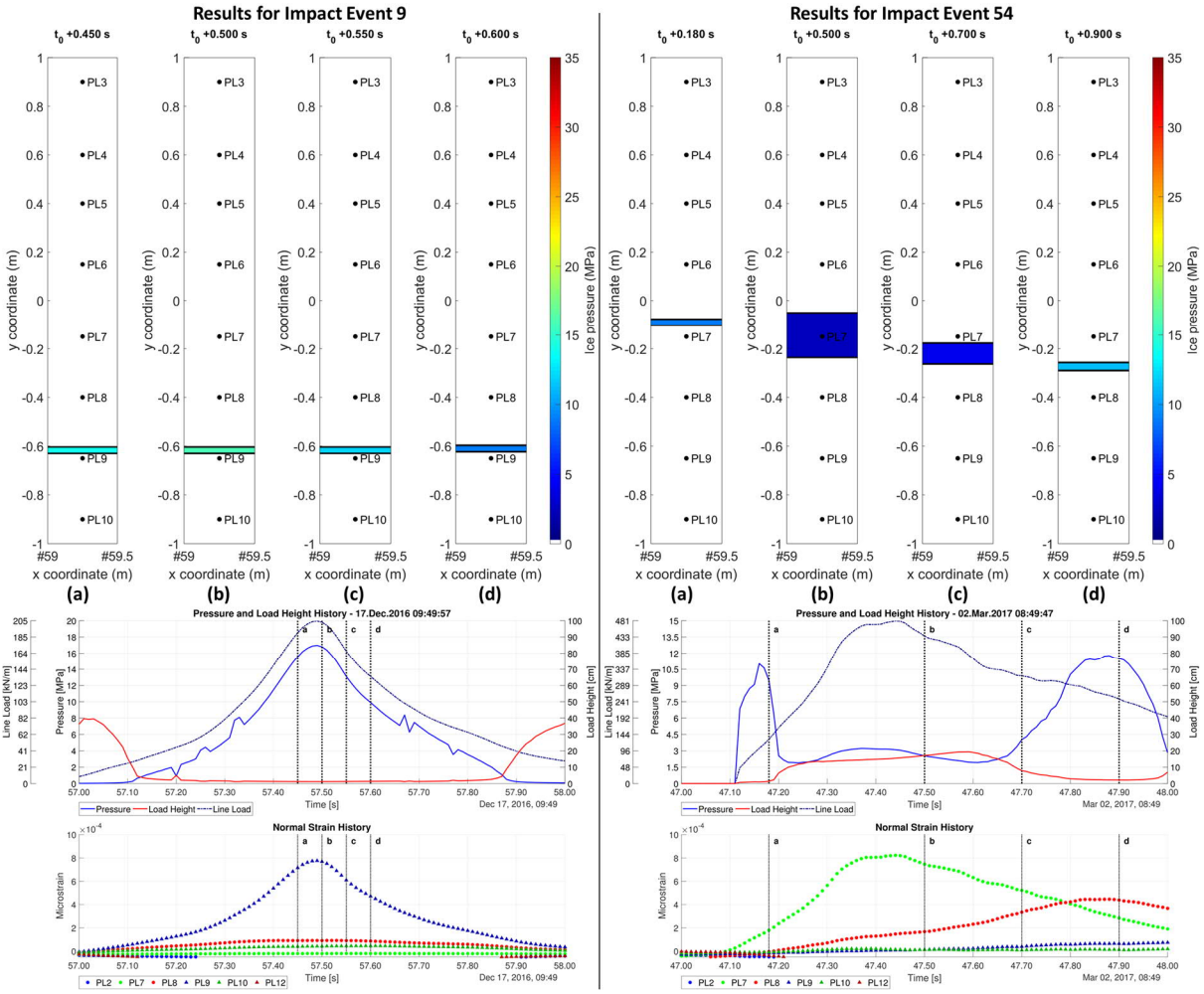

Figure 12. Full time history of two sample impact events

CONCLUSIONS

An inverse method was developed and implemented to study the pressure and load patches induced during ship-ice interactions. Full-scale strain measurement data collected on board the icebreaker *Baltika* was analysed.

The results from the general analysis of 166 impact events reveal that the peak pressures induced during ship-ice interaction are most often between 10 and 25 MPa. Furthermore, the pressure is acting over a narrow area with a height of 1-3 cm. The results align well with visual observations made in the 1990s.

The detailed analysis of individual impact events showed markedly constant load heights throughout the duration of the impact events. The individual impact events also showed the complete development of pressure throughout the 1-second long interactions.

The systematic study of approximately 350 impact events demonstrates that inverse methods are a functional tool for analysing ship-ice interaction. Further improvements to the method are possible to allow for flexibility in the shape of the identified load patch and the identification of potential low pressure contacts surrounding the dominant pressure patch identified in this method. Furthermore, the implications of the higher, more concentrated loads on structural design should be investigated.

REFERENCES

Adams, J., 2018. *Application of an Extended Inverse Method for the Determination of Ice-induced Loads on Ships.* Master's thesis. Espoo, Finland: Aalto University .

Gagnon, R., 2008. Analysis of Data from Bergy Bit Impacts Using a Novel Hull-mounted External Impact Panel. *Cold Regions Science and Technology,* 52(1), pp. 50-66.

Ikonen, T., 2013. *Inverse Ice-induced Load Determination on the Hull of an Ice-going Vessel.* Master's thesis. Espoo, Finland: Aalto University.

Kujala, P. & Vuorio, J., 2009. *On the Statistical Nature of Ice-induced Pressures Measured On Board I.B. Sisu.* Luleå, Sweden, Proceedings of the 20th International Conference on Port and Ocean Engineering Under Arctic Conditions.

Kujala, R., 2017. *Ice Strengthing Rules.* [Lecture Notes] Espoo, Finland: Aalto University .

Leira, B., Børsheim, L., Espeland, Ø. & Amdahl, J., 2009. Ice-load Estimation for a Ship Hull Based on Continuous Response Monitoring. *Journal of Engineering for the Maritime Environment,* 223(4), pp. 529-540.

Ochi, M., 1981. *Principles of Extreme Value Statistics and their Application.* Extreme Loads Response Symposium. Arlington, USA, The Society of Naval Architects and Marine Engineers, pp. 15-30.

Riska, K., 1991. *Observations of the Line-like Nature of Ship-ice Contact.* St. John's, Canada, 11th International Conference on Port and Ocean Engineering Under Arctic Conditions, vol. 2, pp. 785-811.

Riska, K. & Kamarainen, J., 2011. A Review of Ice Loading and the Evolution of the Finnish-Swedish Ice Class Rules. *SNAME Annual Meeting,* pp. 1-44.

Riska, K., Rantala, K. & Joensuu, A., 1990. *1990/M97 Full Scale Observations of Ship-Ice Contact,* Espoo, Finland: Helsinki University of Technology, Ship Laboratory.

Romppanen, A.-J., 2008. *Inverse Load Sensing Method for Line Load Determination of Beam-like Structures.* Ph.D. dissertation. Tampere, Finland: Tampere University of Technology.

Suominen, M., 2018. *Uncertainty and Variation in Measured Ice-Induced Loads on a Ship Hull.* Ph.D. Espoo, Finland: Aalto University.

Suominen, M. & Kujala, P., 2015. *The Measured Line Load as Function of the Load Length in Antarctic Waters.* Trondheim, Norway, 23rd International Conference on Port and Ocean Engineering under Arctic Conditions.

Tikhonov, A. & Arsenin, V., 1977. *Solution of Ill-Posed Problems.* Washington, DC, USA: Winston and Sons.

Uhl, T., 2007. The Inverse Identification Problem and its Technical Application. *Archive of Applied Mechanics,* Volume 77, pp. 325-337.